Low-Temperature Epitaxial Growth of the Quaternary Wide Band Gap Semiconductor SiCAlN

R. Roucka,[1] J. Tolle,[2] A. V. G. Chizmeshya,[3] P. A. Crozier,[3] C. D. Poweleit,[1] D. J. Smith,[1,3]
I. S. T. Tsong,[1] and J. Kouvetakis[2]

[1]*Department of Physics and Astronomy, Arizona State University, Tempe, Arizona 85287*
[2]*Department of Chemistry and Biochemistry, Arizona State University, Tempe, Arizona 85287*
[3]*Center for Solid State Science, Arizona State University, Tempe, Arizona 85287*
(Received 28 November 2001; published 2 May 2002)

Two compounds SiC and AlN, normally insoluble in each other below ~2000 °C, are synthesized as a single-phase solid-solution thin film by molecular beam epitaxy at 750 °C. The growth of epitaxial SiCAlN films with hexagonal structure takes place on 6H-SiC(0001) substrates. Two structural models for the hexagonal SiCAlN films are constructed based on first-principles total-energy density functional theory calculations, each showing agreement with the experimental microstructures observed in cross-sectional transmission electron microscopy images. The predicted fundamental band gap is 3.2 eV for the stoichiometric SiCAlN film.

DOI: 10.1103/PhysRevLett.88.206102 PACS numbers: 81.15.Hi, 68.37.Lp, 68.55.Jk

In recent years, semiconductors with band gaps >2.0 eV, generally known as wide band gap semiconductors, have found many useful optoelectronic and microelectronic applications. These materials include silicon carbide (SiC), gallium nitride (GaN), and other Group-III nitride ternary alloys. In spite of their successes, a number of fundamental problems remain, among them are the high temperatures involved in their synthesis and the high defect density associated with the material. In this Letter, we demonstrate that these problems can, to a large extent, be alleviated by the epitaxial growth of the quaternary semiconductor alloy SiCAlN.

Both SiC and AlN have hexagonal structures, although SiC also exists in cubic form. In the 2H-wurtzite form, the lattice-parameter mismatch is very small (2H-SiC: $a = 3.08$ Å, $c = 5.04$ Å; AlN: $a = 3.11$ Å, $c = 4.98$ Å), and both are wide band gap semiconductors, 3.3 eV for 2H-SiC and 6.3 eV for AlN. They also share similar physical properties, including mechanical hardness [1] and thermal expansion [2,3]. It would be highly rational, therefore, to attempt to grow a SiCAlN alloy film, in view of the potential applications, in electronic devices as well as lightweight superhard coatings. Unfortunately, the task is made difficult by the fact that a solid solution of SiC and AlN can only form above 1900 °C, based on earlier studies of fabrication of ceramic alloys in the $(SiC)_{1-x}(AlN)_x$ system by hot pressing [4,5]. The miscibility gap extends from $x = 0.15$ to $x = 0.85$, implying that SiC and AlN will segregate into separate phases at temperatures below 1900 °C [6]. However, $(SiC)_{1-x}(AlN)_x$ solid-solution films have been synthesized under metastable growth conditions using molecular beam epitaxy (MBE) [7,8] and metalorganic chemical vapor deposition (MOCVD) methods [9] at temperatures 1000–1300 °C. Because of the complexities encountered in the growth process, i.e., adjustment of four independent flux species in various forms of gases, plasmas, and atomic vapors, coupled with high growth temperatures, little progress in the growth of $(SiC)_{1-x}(AlN)_x$ films has been made since these initial studies.

In this Letter, we describe a small lattice-mismatch heteroepitaxial growth process based upon thermally activated reactions on a 6H-SiC(0001) substrate between a unimolecular precursor source of H_3SiCN vapor and Al atoms from an effusion cell to initiate growth of a stoichiometric SiCAlN film. The film growth takes place in an MBE chamber with the substrate held at 750 °C, far below the miscibility gap temperature of 1900 °C. The precursor was synthesized via a single-step process by a direct combination reaction of SiH_3Br and AgCN. The resulting compound, H_3SiCN, is a stable and highly volatile solid with a vapor pressure of 300 Torr at room temperature, making it highly suitable as a gas source for film growth by MBE. When combined with an Al-atom flux from an effusion cell, the epitaxial growth of stoichiometric SiCAlN on a 6H-SiC(0001) substrate proceeds via the chemical reaction:

$$2H_3SiCN\ (gas) + 2Al\ (atoms) \rightarrow 2SiCAlN\ (film) + 3H_2\ (gas).$$

The base pressure in the MBE growth chamber was 2×10^{-10} Torr. The Si-terminated 6H-SiC(0001) substrate was prepared by high-temperature hydrogen etching followed by brief flashing to 1000 °C to produce a $(\sqrt{3} \times \sqrt{3})$ reconstructed surface [10]. The H_3SiCN precursor was delivered via a nozzle positioned 2 cm away from the substrate surface. During film growth, the chamber pressure rose to 5×10^{-7} Torr. The flux rate of each species was varied between 7×10^{13} and 3×10^{14} $cm^{-2}\,s^{-1}$, while the flux ratio of H_3SiCN:Al was maintained at ~1. Under these conditions, the growth rate of the SiCAlN film at 750 °C was ~4 nm/min. The films grown on 6H-SiC(0001) substrates have a transparent appearance, as expected for a wide band gap semiconductor.

The composition of the SiCAlN films grown at 750 °C was studied by Rutherford backscattering spectrometry (RBS) and high-resolution electron-energy-loss spectroscopy (EELS). The RBS results give a composition in atomic percent of (27 ± 1)% for Si, (23 ± 1)% for Al, (25 ± 2)% for C, and (25 ± 2)% for N, suggesting a closely stoichiometric SiCAlN compound. Since, under thermodynamic equilibrium conditions, SiC and AlN are mutually insoluble at 750 °C [6], we used high-resolution EELS with a 1 nm probe diameter to examine the possibility of phase separation in the SiCAlN films. In all the films examined, each nanometer-scale region probed by EELS consistently showed the occurrence of all four constituent elements, Si, Al, C, and N, without any indication of phase separation of SiC and AlN or any segregation of individual elements, thus confirming that the films contained a solid solution of SiCAlN. These EELS results are similar to those obtained earlier on superhard SiCAlN films grown on Si(111) substrates [11].

The microstructure of the SiCAlN films was studied by cross-sectional transmission electron microscopy (XTEM). The lattice parameters of the films are $a = 3.08 \pm 0.03$ Å and $c = 4.98 \pm 0.06$ Å determined from digital diffractograms of XTEM images. The low-resolution XTEM image in Fig. 1(a) shows that the film consists of a columnar microstructure, with the columns aligned with the growth axis {0001}, indicative of predominantly (0001) basal plane growth for the films. The surface morphology of these films shown in atomic force microscopy (AFM) images in Fig. 2 contains features that also suggest that film growth proceeds via coalescence of columns. Analysis of XTEM and AFM images shows that the columns have widths between 20 and 100 nm. In this respect, the columnar microstructure of SiCAlN grown on 6H-SiC(0001) substrates shares some similarities with the Group-III nitride films grown by MOCVD reported in literature [12]. A typical x-ray rocking curve taken on the SiCAlN film is shown in Fig. 3. The reasonably narrow 73.6 arcsec at full width at half maximum (FWHM) of the rocking curve indicates a small mosaic spread of the columns composing the film, in agreement with the observations in XTEM as exemplified by Fig. 1(a).

The high-resolution XTEM image in Fig. 1(b) shows clearly the transition at the interface from the 6H hexagonal structure of the SiC(0001) substrate to an apparent 2H-wurtzite structure of the SiCAlN film. Upon closer inspection, however, in spite of the almost perfect registry at the interface, the microstructure of the SiCAlN film itself is not uniquely defined. We have selected two regions of the film, outlined in Fig. 1(b) by white rectangles labeled *A* and *B*, for computer image simulation of the microstructure [13]. The results of the high-resolution image matching are shown in Fig. 4. Figure 4A shows matching between the experimental XTEM image and the computer simulated image based on a structure consisting of 2H-SiC and 2H-AlN or 2H/2H alternating layers (Fig. 4A), while

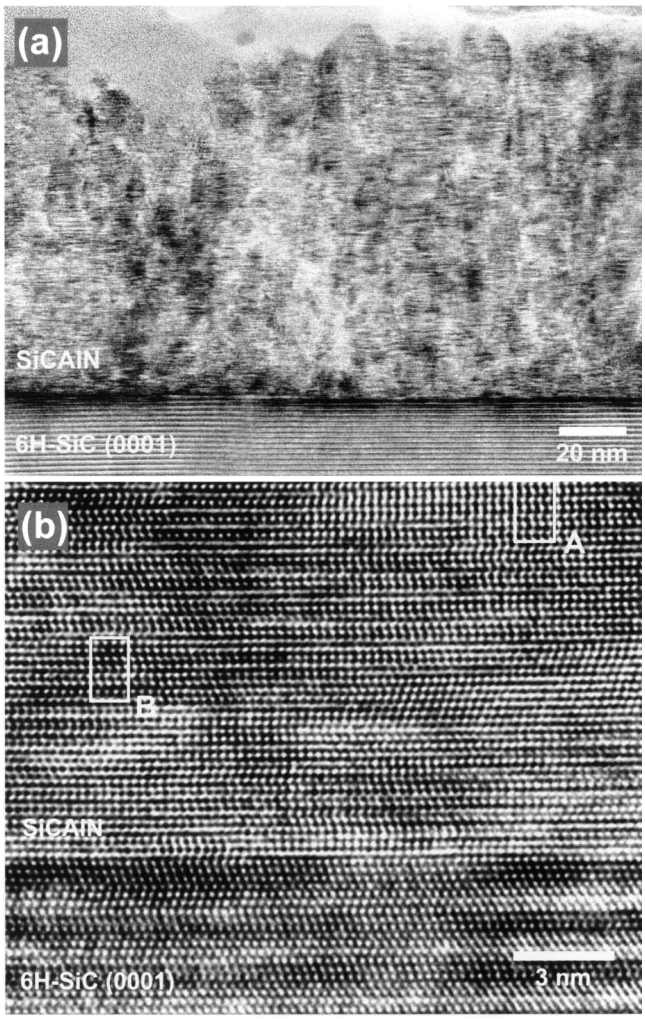

FIG. 1. (a) An XTEM image showing the columnar texture of the SiCAlN epitaxial film grown on a 6H-SiC(0001) substrate at 750 °C. (b) A high-resolution XTEM image showing the interface between the epitaxial wurtzite SiCAlN film and the 6H-SiC(0001) substrate. Two regions outlined by rectangles *A* and *B* are selected for computer-simulated image matching.

image matching in Fig. 4B shows agreement with a structure of 4H/2H alternating layers, i.e., 4H-SiC and 2H-AlN (Fig. 4B). We have also simulated a 4H/4H structure, but could not identify in the XTEM image any region that matches a 4H/4H structure. While it is well known that SiC has several polytypes, AlN, on the other hand, is only known to exist in the 2H-wurtzite form in ambient conditions. Thus it may not be surprising that the microstructure of the films does not contain the 4H/4H structure.

To elucidate our observations, we conducted a first-principles simulation study of $(SiC)_{1-x}(AlN)_x$ solid-solution models. These were generated by combining 2H and 4H unit-cell structures of both SiC and AlN within a single 32-atom, 8 double-layer orthorhombic supercell, as shown in Fig. 4. All properties were computed using a plane-wave pseudopotential method within the Perdew-Burke-Ernzerhof generalized gradient approximation (PBE-GGA) of density functional theory

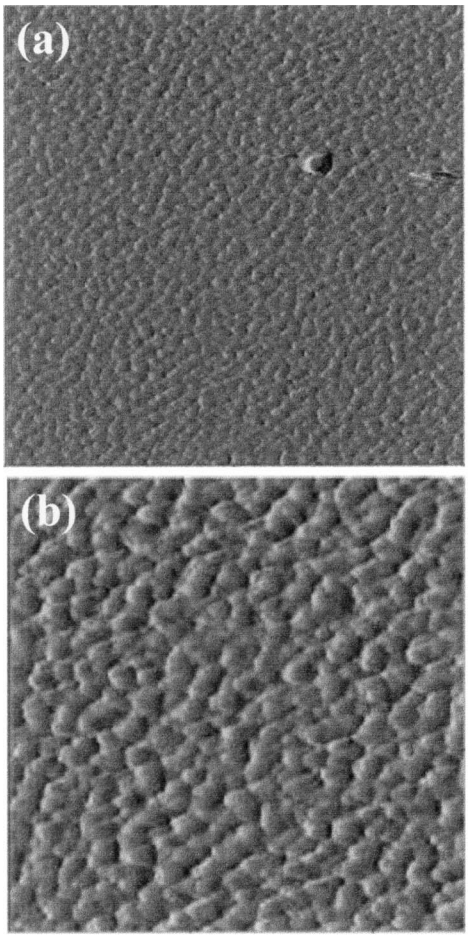

FIG. 2. AFM images of SiCAlN film showing scanned areas of (a) $5.0 \times 5.0\ \mu m^2$ and (b) $2.5 \times 2.5\ \mu m^2$. rms roughness of the surface is ~6.0 nm.

(DFT) [14,15]. To reduce systematic errors, all bulk energies were calculated in exactly the same way using the same supercell with a plane-wave kinetic energy cutoff of 50 Ry, and four irreducible **k** points for the Brillouin-zone integrations. Structures were optimized with respect to both volume and lattice-constant c/a ratio variation, while the interlayer spacing was approximated by the "Vegard" average for the 2H-SiC and 2H-AlN structures using the internal parameter $u \sim 0.378$ for the wurtzite structure [16]. While this approach neglects small variations of ~0.01–0.02 Å in the bond lengths along the c-axis direction relative to fully relaxed calculations, our calculated bulk properties for 2H-SiC, 4H-SiC, 2H-AlN, and 4H-AlN agree well with previous calculated and measured values, e.g., within 2%–4% for lattice constants, and within ~1% for cohesive energies. We also find the 4H-SiC polytype to be more stable than its 2H counterpart by 4 meV/atom, while the energy of the 2H-AlN is 8 meV/atom lower than that of 4H-AlN structure.

Formation energies were computed as the difference between the static lattice ground-state energy of $(SiC)_{1-x}(AlN)_x$ and a reference state consisting of the most stable polytype phases, i.e., 4H-SiC and 2H-AlN. We obtain 50 meV/atom for both the 2H/2H and 4H/2H model structures of SiCAlN shown in Fig. 4, and about 52 meV/atom for the 4H/4H structure (not shown). These energies differ by only a few meV per atom; a value typical of the polytype energy differences found in SiC [17], suggesting that solid solutions exhibiting these motifs may readily form. We also find that supercells containing mixed bonds, e.g., Al-C or Si-N, within a double layer, are far less energetically favorable (with a calculated formation energy of 198 meV/atom for a mixed bond 2H/2H-type model) and therefore these are excluded in our consideration. Our calculated formation energies correspond to ordered heterostructures containing Al-C and Si-N bonds only between the double layers, as shown in Fig. 4. The formation energies of the SiC-AlN wurtzite-based alloys considered here are considerably smaller than that given for the cubic form, which is ~200 meV/atom [18]. Random stacking of ordered supercells in a manner that preserves the average composition yields a disordered model whose average properties can be determined using the statistical cluster approach of Connolly and Williams [19].

The band gap behavior with respect to composition for $(SiC)_{1-x}(AlN)_x$ is shown in Fig. 5, indicating a significant band gap bowing effect similar to that predicted in related systems [20–23]. Our calculated GGA band gaps for the

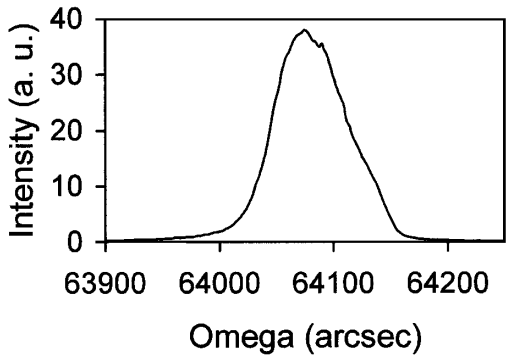

FIG. 3. X-ray rocking curve of an on-axis SiCAlN (002) peak showing a FWHM of 73.6 arcsec.

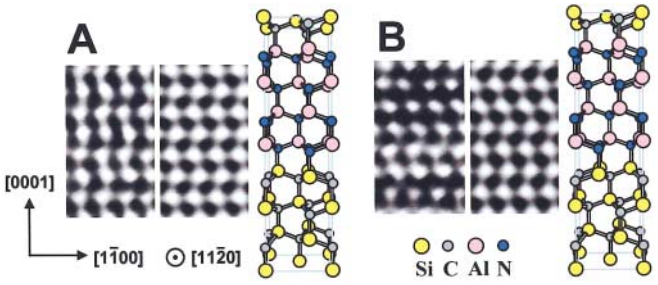

FIG. 4 (color). Comparison of XTEM image (left) of region *A* in Fig. 1(b) with a computer-simulated image (right) based on the SiCAlN structure comprising unit cells of 2H-SiC and 2H-AlN. (B) Comparison of XTEM image (left) of region *B* in Fig. 1(b) with computer-simulated image (right) based on the SiCAlN structure comprising unit cells of 4H-SiC and 2H-AlN.

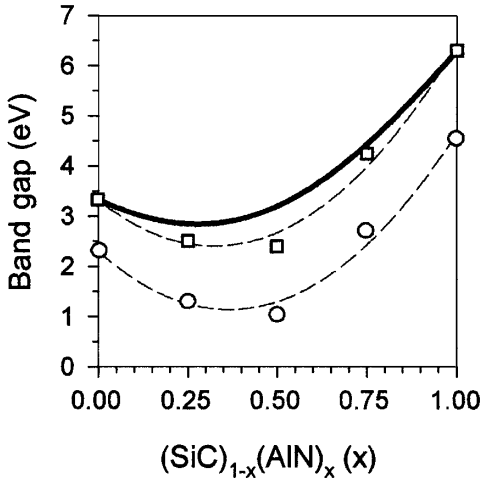

FIG. 5. Theoretically predicted band gap dependence on $(SiC)_{1-x}(AlN)_x$ composition for the ordered and disordered solid-solution models. GGA calculations for the individual ordered heterostructure models are shown in circles; and GGA band gaps corrected to reproduce measured end-member values are shown in squares. The dashed curves are quadratic fits to the GGA and corrected GGA data. The bold solid curve shows corrected GGA data including the Connolly-Williams disorder correction.

end members are $E_g \sim 2.31$ eV for 2H-SiC and 4.54 eV for 2H-AlN, in agreement with other reports [24,25], but they are 1.02 and 1.74 eV lower than the respective measured E_g values. It is well known that the GGA underestimates the band gap in these materials. We compensate for this defect by correcting our computed band gap energies by adding the factor $\Delta E_g(x) = 1.02(1 - x) + 1.74x$ to estimate the values across the entire composition range. To treat the effect of disorder on our corrected $E_g(x)$ curve (marked by squares) in Fig. 5, we adopt the Connolly-Williams approach [19], as suggested by Lambrecht and Segall [18]. This produces a maximum positive disorder correction of about 0.53 eV at the stoichiometric SiCAlN composition, yielding a predicted fundamental band gap of about 3.2 eV indicated by the bold curve in Fig. 5. Room-temperature photoluminescence measurements conducted on SiCAlN films using a He-Cd laser produced a prominent luminescence peak at 3.20 eV with 0.65 eV FWHM, in good agreement with theory.

In summary, we have reported a simple growth method to produce single-phase SiCAlN solid-solution films at 750 °C. The stoichiometric film has a predominantly wurtzite structure comprising unit cells of 2H-SiC/2H-AlN and 4H-SiC/2H-AlN, with a predicted band gap of 3.2 eV. The variation of band gap with composition shown in the bold curve in Fig. 5 suggests that band gap engineering between 3.2 and 4.5 eV is attainable simply by increasing the AlN content in the film from 50% to 75% by the addition of an N-atom flux while simultaneously increasing the Al flux. Our experimental approach involving the combination of a custom-designed unimolecular precursor and metal atoms provides a direct way to grow new quaternary semiconductors in the *XCZN* family, where *X* is a Group-IV metal and *Z* is a Group-III metal. Hypothetical semiconductors with adjustable band gaps, e.g., GeCGaN, are within reach.

This work was supported by the U.S. Army Research Office (Grant No. DAAD19-00-1-0471) and by the National Science Foundation (Grant No. 9986271).

[1] D. M. Teter, MRS Bull. **23**, 22 (1998).
[2] H. Morkoç, S. Strite, G. B. Gao, M. E. Lin, B. Sverdlov, and M. Burns, J. Appl. Phys. **76**, 1363 (1994).
[3] S. Tanaka, R. S. Kern, and R. F. Davis, Appl. Phys. Lett. **66**, 37 (1995).
[4] R. Ruh and A. Zangvil, J. Am. Ceram. Soc. **65**, 260 (1982).
[5] W. Rafaniello, M. R. Plichta, and A. V. Virkar, J. Am. Ceram. Soc. **66**, 272 (1983).
[6] A. Zangvil and R. Ruh, J. Am. Ceram. Soc. **71**, 884 (1988).
[7] R. S. Kern, L. B. Rowland, S. Tanaka, and R. F. Davis, J. Mater. Res. **13**, 1816 (1998).
[8] R. S. Kern, L. B. Rowland, S. Tanaka, and R. F. Davis, J. Mater. Res. **13**, 1816 (1998).
[9] I. Jenkins, K. G. Irvine, M. G. Spencer, V. Dmitriev, and N. Chen, J. Cryst. Growth **128**, 375 (1993).
[10] C. W. Hu, D. J. Smith, R. B. Doak, and I. S. T. Tsong, Surf. Rev. Lett. **7**, 565 (2000), and references therein.
[11] R. Roucka, J. Tolle, D. J. Smith, P. Crozier, I. S. T. Tsong, and J. Kouvetakis, Appl. Phys. Lett. **79**, 2880 (2001).
[12] F. A. Ponce, MRS Bull. **22**, 51 (1997).
[13] Cerius^2 Software Package, Accelyrys Inc., San Diego, California, 2001.
[14] M. Bockstedte, A. Kley, J. Neugebauer, and M. Scheffler, Comput. Phys. Commun. **107**, 187 (1997).
[15] M. Fuchs and M. Scheffler, Comput. Phys. Commun. **119**, 67 (1999).
[16] The wurtzite u parameter is the ratio of the axial (c-axis) bond length, b_A, to the c-axis length, c_H, i.e., $u = b_A/c_H$. The Vegard average u for the two wurtzite structures 2H-SiC and 2H-AlN is defined as $\frac{1}{2}(b_A^{\mathrm{SiC}}/c_H^{\mathrm{SiC}} + b_A^{\mathrm{AlN}}/c_H^{\mathrm{AlN}})$.
[17] S. Limpijumnong and W. R. L. Lambrecht, Phys. Rev. B **57**, 12 017 (1998).
[18] W. R. L. Lambrecht and B. Segall, Phys. Rev. B **43**, 7070 (1991).
[19] J. W. D. Connolly and A. R. Williams, Phys. Rev. B **27**, 5169 (1983).
[20] J.-C. Zheng, H. Q. Wang, C. H. A. Haun, and A. T. S. Wee, J. Phys. Condens. Matter **13**, 5295 (2001).
[21] S. Matsumoto, H. Yaguchi, S. Kashiwase, T. Hashimoto, S. Yoshida, D. Aoki, and K. Onabe, J. Cryst. Growth **221**, 481 (2000).
[22] M. Goano, E. Bellotti, E. Ghillino, C. Garetto, G. Ghione, and K. F. Brennan, J. Appl. Phys. **88**, 6476 (2000).
[23] L. Bellaiche, S.-H. Wei, and A. Zunger, Phys. Rev. B **54**, 17 568 (1996).
[24] C. Persson and U. Lindefelt, Phys. Rev. B **54**, 10 257 (1996).
[25] C. Stampfl and C. G. Van de Walle, Phys. Rev. B **59**, 5521 (1999).